

Dissociation of I_2 and the vibrational kinetics in the oxygen-iodine medium

V N Azyazov, V S Safonov, N I Ufimtsev

Abstract. The comparative analysis of the processes responsible for dissociation of molecular iodine in the oxygen-iodine medium is made. The rate of relaxation of vibrationally excited oxygen in the $O_2-I_2-H_2O$ medium is shown to be limited by the VV energy exchange between oxygen and water molecules, and the fraction of vibrationally excited O_2 ($v = 1$) in the active medium of the oxygen-iodine laser can reach several tens of percent. It is noted that the VV exchange in $O_2(^1\Delta, v = 1) + I(^2P_{3/2}) \leftrightarrow O_2(^3\Sigma, v = 1) + I(^2P_{1/2})$ reaction may be of considerable importance in the kinetics of formation of the active medium in the oxygen-iodine laser.

1. Introduction

Relaxation of the electronic energy accumulated by singlet oxygen in the active medium of the chemical oxygen-iodine laser (COL) causes nonequilibrium population of vibrational levels of O_2 , I_2 , and H_2O molecules. This energy can have a substantial effect on the kinetics of processes in the active medium of a COL, especially the processes associated with dissociation of molecular iodine. Although dissociation of I_2 in singlet oxygen is not yet completely studied, it is well known to be governed by chain and two-step mechanisms. The I_2 molecule cannot dissociate in a single collision with electronically excited oxygen $O_2(^1\Delta)$ or atomic iodine $I(^2P_{1/2})$ because their excitation energies are much smaller than the dissociation energy. The dissociation of I_2 requires at least two photons emitted by electronically excited $O_2(^1\Delta)$. As found experimentally in [1, 2], an increase in the I_2 concentration in a mixture with a fixed content of singlet oxygen reduces the dissociation time. This is evidence of the chain mechanism of dissociation. Therefore, any model of iodine dissociation should include initiation and chain stages.

It was found in Ref. [3] that molecular iodine rapidly dissociates in the presence of singlet oxygen. In this paper, two possible models of iodine dissociation were proposed. In the first model (model I, Table 1), where electronically excited oxygen $O_2(^1\Sigma)$ plays an important role, iodine dissociates in accordance with reactions 1–4 (Table 1). At the initiation

stage, $O_2(^1\Sigma)$ is produced in reaction 1. At the chain stage, after the production of a certain amount of atomic iodine, $O_2(^1\Sigma)$ is produced in reaction 4. In the second model (model II), an iodine molecule dissociates after two successive collisions with $O_2(^1\Delta)$ in reactions 5a and 6a. Based on the analysis of their experimental data, the authors of Refs [4–6] concluded that iodine dissociated in accordance with model I. A satisfactory agreement between the calculations and the experimental results was obtained when the rate constant of reaction 2 was $K_2 = 2 \times 10^{-10} \text{ cm}^3 \text{ s}^{-1}$. The rate constant directly measured in Ref. [7] proved to be much smaller than expected value. Model II was not widely applied because it did not take into account the chain dissociation mechanism.

The analysis of experimental data on iodine dissociation shows that reactions 4 and 7 are the only reactions in the oxygen-iodine medium that are able to provide the necessary dissociation rates at the chain stage. At the initiation stage, reaction 1 has the highest rate, but it does not provide the required dissociation rate.

The dissociation model that is most extensively used nowadays has been proposed in Ref. [1] (model III). This model is characterised by the population of an intermediate state of the I_2^* dissociation at the chain stage in reaction 7. This state is not concretised there. It was assumed to be either the electronically excited $I_2(A'^3\pi_{2u})$ state of molecular iodine or the vibrationally excited ground electronic state of iodine $I_2(X, 30 \leq v \leq 40)$ (Fig. 1). The intermediate iodine state relaxes in accordance with reactions 8–10. In reaction 6b, which is similar to reaction 6a from model II, the dissociative iodine terms are populated from an intermediate I_2^* state. In Refs [20–22], population of vibrational levels of $I_2(X)$ in singlet oxygen was studied. The population of vibrational iodine levels with $v = 30–45$ was shown to be substantially nonequilibrium. Based on this fact, the authors of Refs [20–22] assumed that vibrationally excited iodine in the ground electronic state $I_2(X, 30 \leq v \leq 40)$ might be an intermediate I_2^* state in iodine dissociation.

To explain the dissociation rates observed at the initiation stage of the dissociation process, reaction 5b was introduced in model III. It remains unclear which energy state of iodine is an intermediate one at the initiation state. All the known rate constants of the $O_2(^1\Delta)$ deactivation by molecules [23] are smaller by several orders of magnitude than the rate of reaction 5b. It is most likely that the rate of EV energy transfer between $O_2(^1\Delta)$ and I_2 is unable to provide the required iodine dissociation rate at the initiation stage. It is more likely that the EE exchange occurs between them. The electronically excited state of molecular iodine that is the nearest one to $O_2(^1\Delta)$ is the $(A'^3\pi_{2u})$ state with the excitation energy of

V N Azyazov, V S Safonov, N I Ufimtsev P N Lebedev Physics Institute, Samara Branch, Russian Academy of Sciences, Novo-Sadovaya ul. 221, 443011 Samara, Russia

Received 10 October 1999; revision received 27 April 2000

Kvantovaya Elektronika 30(8) 687–693 (2000)

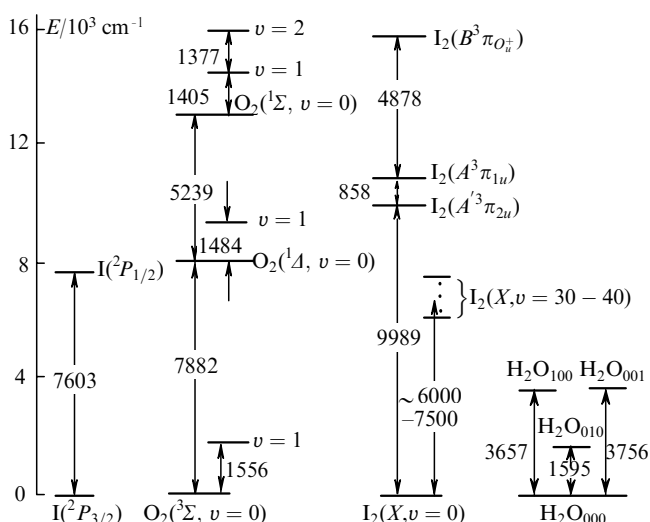
Translated by A N Kirkin; edited by M N Sapozhnikov

Table 1. Rate constants of reactions in the oxygen-iodine medium.

Dissociation model	Reaction number j	Reaction	Rate constant $K_j/\text{cm}^3 \text{ s}^{-1}$	References
I [3]	1	$\text{O}_2(^1\text{A}) + \text{O}_2(^1\text{A}) \rightarrow \text{O}_2(^1\Sigma, v) + \text{O}_2(^3\Sigma)$	$9.5 \times 10^{-28} T^{3.8} \exp(700/T)$	[8]
	2	$\text{O}_2(^1\Sigma) + \text{I}_2 \rightarrow \text{O}_2(^3\Sigma) + 2\text{I}(^2\text{P}_{3/2})$	4×10^{-12}	[7]
	2a	$\text{O}_2(^1\Sigma, v=2) + \text{I}_2 \rightarrow \text{O}_2(^3\Sigma) + 2\text{I}(^2\text{P}_{3/2})$	2×10^{-10}	
	3	$\text{O}_2(^1\text{A}) + \text{I}(^2\text{P}_{3/2}) \leftrightarrow \text{O}_2(^3\Sigma) + \text{I}(^2\text{P}_{1/2})$	$K_{\text{eq}} 0.75 \exp(402/T)$	[9]
	4	$\text{I}(^2\text{P}_{1/2}) + \text{O}_2(^1\text{A}) \rightarrow \text{I}(^2\text{P}_{3/2}) + \text{O}_2(^1\Sigma, v)$	$4 \times 10^{-24} T^{3.8} \exp(700/T)$	[8]
II [3]	5a	$\text{O}_2(^1\text{A}) + \text{I}_2(\text{X}) \rightarrow \text{O}_2(^3\Sigma) + \text{I}_2(\text{A}'^3\pi_{2u})$		
	6a	$\text{O}_2(^1\text{A}) + \text{I}_2(\text{A}'^3\pi_{2u}) \rightarrow \text{O}_2(^3\Sigma) + 2\text{I}(^2\text{P}_{3/2})$		
	5b	$\text{O}_2(^1\text{A}) + \text{I}_2(\text{X}) \rightarrow \text{O}_2(^3\Sigma) + \text{I}_2^*$	7×10^{-15}	[1]
III [1]	6b	$\text{O}_2(^1\text{A}) + \text{I}_2^* \rightarrow \text{O}_2(^3\Sigma) + 2\text{I}(^2\text{P}_{3/2})$	3×10^{-11}	[1]
	7	$\text{I}(^2\text{P}_{1/2}) + \text{I}_2(\text{X}) \rightarrow \text{I}(^2\text{P}_{3/2}) + \text{I}_2^*$	3×10^{-11}	[10]
	8	$\text{I}_2^* + \text{O}_2(^3\Sigma) \rightarrow \text{I}_2(\text{X}) + \text{O}_2(^3\Sigma)$	5×10^{-12}	[1]
	9	$\text{I}_2^* + \text{Ar} \rightarrow \text{I}_2(\text{X}) + \text{Ar}$	2.3×10^{-11}	[20]
	10	$\text{I}_2^* + \text{H}_2\text{O} \rightarrow \text{I}_2(\text{X}) + \text{H}_2\text{O}$	3×10^{-10}	[1]
	5c	$\text{O}_2(^1\text{A}, v=1) + \text{I}_2(\text{X}) \rightarrow \text{O}_2(^3\Sigma) + \text{I}_2(\text{A}'^3\pi_{2u})$	1.4×10^{-11}	
	11	$\text{O}_2(^1\Sigma) + \text{H}_2\text{O} \rightarrow \text{O}_2(^1\text{A}, v) + \text{H}_2\text{O}(v)$	6.7×10^{-12}	[12]
IV [11]	12	$\text{O}_2(^1\text{A}, v) + \text{O}_2(v') \leftrightarrow \text{O}_2(^1\text{A}, v-1) + \text{O}_2(v'+1)$	$\sim 10^{-12}$	[13, 14]
	13	$\text{O}_2(v=1) + \text{H}_2\text{O}(000) \leftrightarrow \text{O}_2(v=0) + \text{H}_2\text{O}(010)$	$\sim 3 \times 10^{-13}$	
	14	$\text{O}_2(v=1) + \text{O}_2 \rightarrow \text{O}_2(v=0) + \text{O}_2$	10^{-18}	[15]
	15	$\text{O}_2(v=1) + \text{Ar} \rightarrow \text{O}_2(v=0) + \text{Ar}$	2×10^{-21}	[16]
	16	$\text{O}_2(v=1) + \text{H}_2\text{O} \rightarrow \text{O}_2(v=0) + \text{H}_2\text{O}$	10^{-16}	[16]
	17	$\text{H}_2\text{O}(010) + \text{H}_2\text{O} \rightarrow \text{H}_2\text{O}(000) + \text{H}_2\text{O}$	5×10^{-11}	[17]
	18	$\text{O}_2(^3\Sigma) + \text{I}(^2\text{P}_{1/2}) \rightarrow \text{O}_2(^3\Sigma, v) + \text{I}(^2\text{P}_{3/2})$	3×10^{-14}	[18]
	19	$\text{H}_2\text{O} + \text{I}(^2\text{P}_{1/2}) \rightarrow \text{H}_2\text{O}(v) + \text{I}(^2\text{P}_{3/2})$	2.3×10^{-12}	[19]
	20	$\text{O}_2(^1\Sigma, v=2) + \text{O}_2 \rightarrow \text{O}_2 + \text{O}_2$	2.7×10^{-12}	[14]
	21	$\text{O}_2(^1\text{A}, v=1) + \text{I}(^2\text{P}_{3/2}) \leftrightarrow \text{O}_2(^3\Sigma, v=1) + \text{I}(^2\text{P}_{1/2})$?		

Note. T is measured in Kelvin; K_{eq} is the reaction equilibrium constant.

9989 cm^{-1} (see the energy level diagram in Fig. 1). The energy gap between these states is $\Delta E = 2107 \text{ cm}^{-1}$. If an $\text{O}_2(^1\text{A})$

**Figure 1.** Some energy levels of the I atom and O_2 , I_2 , and H_2O molecules.

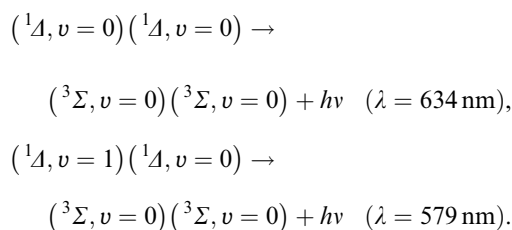
molecule is found at the first vibrational level, ΔE in reaction 5a is considerably smaller (623 cm^{-1}).

As shown in Ref. [11], the electronic-energy relaxation in the active medium of the COL causes a substantially non-equilibrium population of vibrational levels of oxygen molecules. In Ref. [11], the iodine dissociation mechanism was proposed in which vibrationally excited oxygen $\text{O}_2(^1\text{A}, v=1)$ plays an important role (model IV). In this model, as in model II, the electronically excited state of molecular iodine $\text{A}'^3\pi_{2u}$ is an intermediate I_2^* state. This state is populated, both at the initiation and chain stages, according to reaction 5c, which is similar to reactions 5a and 5b. A distinctive feature of model IV is that dissociation at all stages is described by the same processes, whereas model III uses different processes. Model IV adequately describes the iodine dissociation rates observed in the experiments [11]. In Ref. [24], the iodine dissociation mechanism involving vibrationally excited singlet oxygen with $v \geq 3$ was proposed. This mechanism can take place in mixtures containing no water vapour.

In this paper, we compare previously proposed models of iodine dissociation in the singlet oxygen medium and determine the vibrational oxygen population at the output of a chemical jet-droplet generator of singlet oxygen in the active medium of the COL.

2. Experiments

The measurement of the vibrational population in the active medium of the COL is a complicated problem [24]. In Ref. [25], a method for determining the vibrational population of oxygen with $v = 1$ in a medium with electronically excited oxygen molecules from the analysis of emission spectra of oxygen dimoles at wavelengths 634 and 579 nm was proposed. Cooperative events of emission of electronically excited oxygen molecules in the bands with centres at these wavelengths are described by the processes



At the wavelength of 579 nm, emission is produced by an oxygen dimole formed by two molecules of singlet oxygen, one of which is vibronically excited with $v = 1$. In Ref. [26], the ratio of rate constants of these processes $K_{579}/K_{634} = 0.93$ is presented. Using the ratio of rates of photon emission in these processes and the experimentally measured radiation intensities at these wavelengths, I_{579} and I_{634} , we can determine the relative population of oxygen at the level $v = 1$ from the relation [27]

$$\frac{[\text{O}_2(^1\Delta, v = 1)]}{[\text{O}_2(^1\Delta, v = 0)]} = \frac{I_{579} K_{634}}{I_{634} K_{579}}, \quad (1)$$

where $[\text{O}_2(^1\Delta, v = 0)]$ and $[\text{O}_2(^1\Delta, v = 1)]$ are the concentrations of singlet oxygen with vibrational quantum numbers $v = 0$ and 1, respectively.

Luminescence spectra of oxygen dimoles at the output of a jet-droplet generator of singlet oxygen were measured on a setup, which is described in detail in Ref. [27]. The generator reaction zone represented a cylindrical cavity 12 mm in diameter and 10 cm high, which was drilled in a block of organic glass. We used a gas-liquid generator operating in the counterflow mode. Gaseous Cl₂ was injected into the lower part of the generator reaction zone, and an alkaline solution of hydrogen peroxide was injected into its upper part. The injector for this solution consisted of 85 pipes made of stainless steel, with an inner diameter of 0.3 mm and a length of 25 mm. The jet velocity in the reactor was $\sim 20 \text{ m s}^{-1}$, and the rate of chlorine flow was 10 mmol s^{-1} . The fraction of O₂(¹Δ) in the gas flow at the output of the singlet oxygen generator was $\sim 65\%$, and the degree of chlorine utilisation under our experimental conditions exceeded 90%.

We used a measurement cell made of organic glass and having a cylindrical channel 10 mm in diameter drilled in it, which was attached directly to the generator block. The pressure and the gas velocity in the measurement cell were 70 Torr and 30 m s^{-1} , respectively. We used an additional injector between the generator and the measurement cell to inject gaseous nitrogen and iodine vapour into the oxygen flow. Radiation was outcoupled from the measurement cell through quartz windows at its ends. The light signal passing through the window was incident on the entrance slit of an MDR-6 monochromator, and the signal outgoing from its exit slit was detected by a FEU-69B photomultiplier. Photo-

detector signals were amplified by a universal precise U7-1 dc amplifier whose transmission band extended from zero to 10 Hz.

Emission spectra of oxygen dimoles were measured in two regimes. In the first regime, the gas was supplied from the output of the singlet oxygen generator through the measurement cell. The gas circuit connecting the generator outlet with the cell inlet represented a cylindrical channel 9 mm in diameter and 45 mm long. In the second regime, we injected iodine vapour into the gas flow from the generator. The vapour was injected at a distance of 25 mm from the cell inlet. The intensity measured ratio for the 634-nm and 579-nm emission bands in the first regime was $I_{579}/I_{634} \approx 0.02$. By substituting this value in (1), we find the relative vibrational population of singlet oxygen at the outlet of the jet-droplet generator

$$\frac{[\text{O}_2(^1\Delta, v = 1)]}{[\text{O}_2(^1\Delta, v = 0)]} \approx 0.02.$$

Thus, approximately 2% of oxygen molecules at the generator outlet are vibrationally excited. The gas temperature in the measurement cell in these experiments was 350 K [27]. At this temperature, the equilibrium concentration of vibrationally excited oxygen is lower than the measured value by an order of magnitude. Vibrational levels of oxygen at the outlet of the singlet oxygen generator are populated in reaction 1. In reaction 12 of the VV exchange (see Table 1), vibrational quanta are redistributed over all the electronic states of oxygen and accumulated at the vibrational level with $v = 1$. The rates of VT relaxation of the vibrational energy accumulated in oxygen are rather low (reactions 14–16), and, therefore, energy transfer from the vibrational reservoir to the thermal one occurs in the following way.

At the first stage in reaction 13, oxygen molecules transfer vibrational quanta to water molecules. At the second stage, the vibrational energy is transformed into translational degrees of freedom of a gas mixture in the rapid reaction 17. The rate of reaction 13 is much lower than the rate of reaction 17, and because of this, it limits the vibrational-energy relaxation rate. The rate constant of this process can be estimated by equating the rate of production of vibrational quanta n_v in reaction 1 to the rate of reaction 13:

$$n_v K_1 [\text{O}_2(^1\Delta)] [\text{O}_2(^1\Delta)] = K_{13} [\text{O}_2(^1\Delta, v = 1)] [\text{H}_2\text{O}].$$

The concentration of water vapour in a gas flow is equal to the saturation vapour concentration at the solution temperature (-10°C); under our experimental conditions, it was $[\text{H}_2\text{O}] \sim 3 \times 10^{16} \text{ cm}^{-3}$. Reaction 1 in combination with fast reaction 11 can produce four or five vibrational quanta of oxygen [24, 28]. Setting $n_v = 4$, $[\text{O}_2(^1\Delta)] \approx 1.3 \times 10^{18} \text{ cm}^{-3}$, and $K_1(T = 350 \text{ K}) = 3.3 \times 10^{-17} \text{ cm}^3 \text{ s}^{-1}$, we obtain the estimate $K_{13} \approx 3 \times 10^{-13} \text{ cm}^3 \text{ s}^{-1}$ for the rate constant.

Using the technique described above, we attempted to measure the vibrational population of O₂ in the oxygen-iodine medium. For this purpose, molecular-iodine vapour was injected into the oxygen flow at the outlet of the singlet oxygen generator, and its fraction in oxygen was varied in a range of 0.1–1%. Emission of molecular iodine at 579 nm overlapped emission of oxygen dimoles at this wavelength. We failed to separate the emission band of oxygen dimoles from the background produced by the iodine emission. The main rate constants of the processes describing the vibrational kinetics of the oxygen-iodine medium are known (see

Table 1), and, therefore, one can calculate the vibrational population of O_2 .

3. Calculations

Consider the flow of an oxygen-iodine medium in a channel of constant cross section with the subsonic velocity and the Mach number satisfying the relation $M^2 \ll 1$ under the assumption of instantaneous mixing. The flow of singlet oxygen $g = N_A U$ varies along the coordinate x according to the law

$$\frac{d(N_A U)}{dx} = -2K_1 N_A N_A - 2K_4 N_A N_1^* - K_{6a} N_A N_{I_2}^* - K_7 N_1^* N_{I_2} - K_{5c} N_A^v N_{I_2} + K_{11} N_{1s} N_w - K_{18} N_{3s} N_1^* - K_{19} N_w N_1^*.$$

where the subscripts A , $1s$, and $3s$ denote oxygen in the electronic states 1A , ${}^1\Sigma$, and ${}^3\Sigma$, respectively; I and I_2 are atomic and molecular iodine; w is water vapour; and $*$ and v mean electronic and vibrational excitations, respectively. The right-hand side of the equation consists of single-type terms describing the rates of bimolecular reactions. In this case, it is advantageous to make a change to the coordinate $\tau = x p_{ox} / U_0$, where p_{ox} is the partial pressure in Torr and U_0 is the initial gas velocity.

Let us move from the concentrations of components N_i to their fractions $\eta_i = g_i / g_{ox}$, where $g_i = N_i U$ is the flow rate of the i th component; U is the gas velocity; and $g_{ox} = N_{ox}^0 U_0 = \text{const}$ is the total oxygen flow rate. Subsonic gas flows with $M^2 \ll 1$ are characterised by the relation $U/U_0 = T/T_0$, where T and T_0 are the current and the initial gas temperatures, respectively. After simple manipulations, we obtain the following equation for the fraction of singlet oxygen

$$\frac{d\eta_A}{d\tau} = \left(-2k_1 \eta_A \eta_A - 2k_4 \eta_A \eta_1^* - k_{6a} \eta_A \eta_{I_2}^* - k_7 \eta_1^* \eta_{I_2} - k_{5c} \eta_A^v \eta_{I_2} + k_{11} \eta_{1s} \eta_w - k_{18} \eta_{3s} \eta_1^* - k_{19} \eta_w \eta_1^* \right) / t^2, \quad (2)$$

where $k_i = K_i n_{ox}$; $t = T/T_0$; and n_{ox} is the O_2 concentration for $p_{ox} = 1$ Torr and $T = T_0$. One can similarly obtain equations for other components of the medium

$$\frac{d(\eta_i)}{d\tau} = \frac{\sum_j k_i \eta_i \eta_j}{t^2}. \quad (3)$$

The fractions of electronically excited oxygen molecules in the ${}^1\Sigma$ state and of vibrationally excited H_2O (010) molecules can be found with a high accuracy from stationary equations. In this model, we took into account the fact that the VV energy exchange between stretching and bending H_2O modes occurs much faster than the VT relaxation of stretching modes [17]. Similarly, the VV exchange between vibrational levels of oxygen occurs faster than their VT relaxation. Because of this, vibrational energy quanta are accumulated predominantly on the lower excited vibrational level of $O_2(v = 1)$ and on the bending mode of H_2O (010) molecules. The fraction of electronically excited atomic iodine $I({}^2P_{1/2})$ in the flow is determined from the equilibrium condition for direct and inverse reactions 3 (Table 1)

$$\eta_1^* = 2(\eta_{I_2}^0 - \eta_{I_2}) \left(1 - \frac{1 - \eta_A}{K_{eq} \eta_A} \right)^{-1}, \quad (4)$$

where K_{eq} is the reaction 3 equilibrium constant.

The gas flow temperature is described by the equation

$$\frac{dT}{d\tau} = \frac{\sum_i q_i k_i \eta_i \eta_j}{c_p t^2 (1+h)}, \quad (5)$$

where q_i is the energy release in the i th reaction; c_p is the molar heat capacity of a gas medium; and h is the degree of dilution with a buffer gas.

The gain α_p of a medium for the ${}^2P_{1/2}(F = 3) \rightarrow {}^2P_{3/2}(F = 4)$ electronic transition of the iodine atom, reduced to an oxygen pressure of 1 Torr, is given by the equation

$$\alpha_p = \frac{\alpha}{p_{ox}} = \frac{7}{24} \sigma n_{ox} \frac{3\eta_1^* - 2(\eta_{I_2}^0 - \eta_{I_2})}{t^{1.5}}, \quad (6)$$

where σ is the cross section for induced emission at the line centre of the given transition.

The knowledge of the composition of a medium $O_2 : O_2({}^1A) : H_2O : I_2 : N_2 = k : l : m : n : s$ and its temperature at the initial moment (O_2 denotes oxygen in all energy states) is sufficient for solving system (2)–(6). The pressure and the initial gas velocity enter into the expression describing the relation between x and τ . The initial fractions of components of the medium are determined from the chosen mixture composition, which is specified by the fractions of singlet oxygen, $\eta_A^0 = l/k$, molecular iodine, $\eta_{I_2}^0 = n/k$, and water vapour, $\eta_w = m/k$. The initial fractions of vibrationally excited oxygen and water molecules correspond to equilibrium populations of these components at the initial gas temperature T_0 . The degree h of oxygen dilution with a buffer gas in Eq. (5) is also determined from the chosen gas composition as $h = s/k$.

Fig. 2 presents the dependences of gain and the fraction of molecular iodine $\varphi = \eta_{I_2} / \eta_{I_2}^0$ in the oxygen-iodine medium on the coordinate τ calculated for the mixture with composition $O_2 : O_2({}^1A) : H_2O : I_2 : N_2 = 1000 : 700 : 50 : 10 : 0$ and the initial gas temperature $T_0 = 300$ K. This composition is typical of the active medium of the oxygen-iodine laser. The parameters of the medium presented in the figure are calculated for three dissociation models.

One can see from Fig. 2 that the dissociation rate of molecular iodine in models III and IV is the same. In model I with the rate constant of reaction 2 equal to $2 \times 10^{-10} \text{ cm}^3 \text{ s}^{-1}$ [15], the dissociation rate is lower at the initiation stage of the process. This is explained by the fact that the rate of the initiating process in models III, IV exceeds the rate of reaction 1, which may be thought of as an initiating process in model I. As a result, the maximum gain of a medium in model I is reached at the coordinate τ that is greater by a factor of about two, whereas the gain coefficients α_p differ insignificantly.

Direct measurements made in Ref. [7] showed that the rate constant of reaction 2, in which I_2 dissociates in collisions with electronically excited oxygen $O_2({}^1\Sigma, v = 0)$, was smaller by several orders of magnitude than the value expected in Ref. [5]. The situation can be saved by the fact that reaction 1 produces predominantly electronically excited oxygen $O_2({}^1\Sigma, v = 2)$ [28]. One can see from Fig. 1 that the energy of this oxygen state is almost equal to the energy of the electronically excited state of molecular iodine $I_2(B^3\pi_{o_g^+})$. Because of this, it is reasonable to assume that the rate constant of iodine dissociation in reaction 2a is close to the gas-kinetic value.

Fig. 2 also presents calculations of the fraction of molecular iodine and gain of a medium in which dissociation of I_2 was described by reaction 2a and relaxation of the oxygen

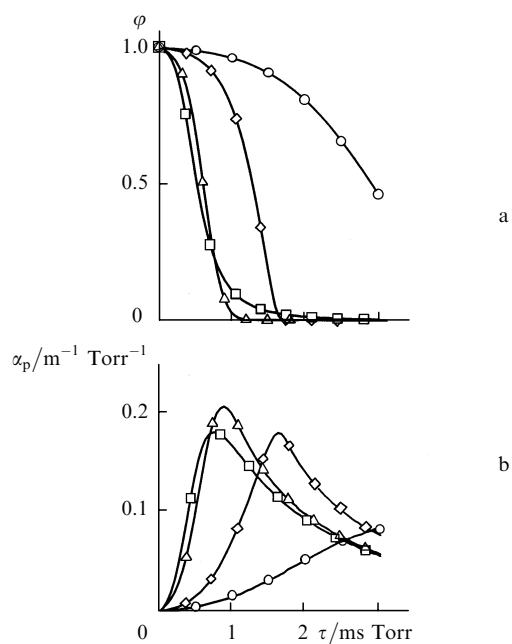


Figure 2. Dependences of the fraction of molecular iodine (a) and the gain coefficient of a medium (b) on the coordinate τ for $T = 300$ K and the medium with composition $\text{O}_2 : \text{O}_2(^1\Delta) : \text{H}_2\text{O} : \text{I}_2 : \text{N}_2 = 1000 : 700 : 50 : 10 : 0$. The calculations are made in the dissociation models presented in Table 1. (Δ) Model IV; (\square) model III; (\diamond) model II; (\circ) model I with reactions 2a, 11, and 20.

state $^1\Sigma$, $v = 2$ was described by reactions 11 and 20. One can see that the dissociation rate in this case is much less than the rate obtained in other models of iodine dissociation analysed by us. Thus, our attempt to reanimate model I failed. In what follows, we analyse only models III and IV.

The second stage of the dissociation process in model IV is reaction 6a. Vibrational levels of oxygen in the oxygen-iodine medium are populated in accordance with reactions 1, 4, 11, and 18. Reactions 14-16 describe the VT exchange between the vibrational and the thermal energy reservoirs. Vibrational energy quanta are redistributed over the oxygen states $^3\Sigma$, $^1\Delta$, and $^1\Sigma$ in quasi-resonant reaction 12, and water vapour is of considerable importance in the vibrational kinetics of the oxygen-iodine medium. In reaction 13, water and oxygen molecules exchange vibrational energy, and reaction 17 is characterised by the highest efficiency of energy transfer from the vibrational reservoir of a mixture to the thermal one.

The concentration of vibrationally excited oxygen in the oxygen flow upstream the iodine injection point is determined by reactions 1, 11, 13, and 17. Under conditions commonly used in the COL, when oxygen pressure is not higher than several Torr, the relationship between relaxation rates for the population of vibrational levels is such that the concentration of $\text{O}_2(^1\Delta, v = 1)$ is close to the equilibrium value. The rate constant of reaction 5c under these conditions was chosen so that the rate constants of reactions 5b and 5c at the initiation stage of the dissociation process in models III and IV be identical. As the number of iodine atoms in the oxygen-iodine medium increases, the rate of population of vibrational oxygen levels in reactions 4, 11, and 18 also increases. As a result, the rate of iodine population to the $A'^3\pi_{2u}$ state also increases. Starting from a certain moment, dissociation passes from the initiation stage to the chain one.

Tables 2 and 3 present parameters of the oxygen-iodine medium for the values of τ corresponding to the maximum gain coefficient of the medium α_p^{\max} for a large set of compositions of the medium. They were calculated in models IV (Table 2) and III (Table 3). For instance, we find from Table 2 that the gain coefficient for the initial gas flow $U_0 = 50$ m s⁻¹, the initial temperature $T_0 = 300$ K, the oxygen pressure $p_{\text{ox}} = 2$ Torr, and the medium with composition $\text{O}_2 : \text{O}_2(^1\Delta) : \text{H}_2\text{O} : \text{I}_2 : \text{N}_2 = 1000 : 700 : 100 : 10 : 0$ reaches its maximum value $\alpha = \alpha_p^{\max} p_{\text{ox}} = 0.348$ m⁻¹ at the point $x = \tau^{\max} U_0 / p_{\text{ox}} = 2$ cm. At this point, the proportion of singlet oxygen is $\eta_A = 0.66$, the proportion of iodine is $\phi = 0.17$, and the gas temperature is $T = tT_0 = 438$ K.

Models III and IV almost similarly describe the dissociation process in a wide range of variation of composition of a medium. An advantage of model IV over model III is that it describes dissociation at the initiation and chain stages by one and the same processes.

Vibrational processes in the oxygen-iodine medium may be important not only in dissociation, but also in the proc-

Table 2. Parameters calculated for the active medium of the oxygen-iodine laser in the transverse section of a gas flow where the gain coefficient reaches a maximum. The calculations are made in model IV for $T_0 = 300$ K and the composition of the medium $\text{O}_2 : \text{O}_2(^1\Delta) : \text{H}_2\text{O} : \text{I}_2 : \text{N}_2 = 1000 : 700 : m : n : 0$.

m	n	$\alpha_p^{\max} / \text{m}^{-1} \text{ Torr}^{-1}$	$\tau^{\max} / \text{ms Torr}$	η_A^{\max}	ϕ^{\max}	t^{\max}
0	1	0.041	2.20	0.69	0.00	1.03
	2	0.080	1.60	0.68	0.00	1.04
	5	0.180	1.13	0.67	0.00	1.09
	10	0.291	0.90	0.66	0.01	1.21
	20	0.366	0.72	0.63	0.03	1.48
10	40	0.316	0.57	0.58	0.16	2.00
	1	0.038	2.00	0.69	0.01	1.08
	2	0.072	1.50	0.69	0.01	1.10
	5	0.154	1.07	0.68	0.03	1.19
	10	0.244	0.85	0.67	0.04	1.33
50	20	0.308	0.68	0.65	0.09	1.61
	40	0.285	0.50	0.61	0.31	2.01
	1	0.035	2.00	0.69	0.02	1.12
	2	0.064	1.50	0.69	0.04	1.16
	5	0.133	1.07	0.68	0.06	1.26
100	10	0.205	0.85	0.66	0.08	1.42
	20	0.263	0.64	0.64	0.18	1.65
	40	0.255	0.50	0.61	0.36	2.05
	1	0.031	2.20	0.68	0.03	1.19
	2	0.056	1.50	0.68	0.08	1.21
200	5	0.113	1.07	0.67	0.10	1.33
	10	0.174	0.80	0.66	0.17	1.46
	20	0.225	0.64	0.64	0.24	1.72
	40	0.229	0.47	0.62	0.45	2.00
	1	0.025	2.20	0.68	0.10	1.27
	2	0.044	1.60	0.67	0.13	1.32
	5	0.087	1.07	0.66	0.20	1.43
	10	0.133	0.80	0.65	0.27	1.56
	20	0.176	0.60	0.64	0.38	1.75
	40	0.192	0.47	0.61	0.51	2.06

Table 3. Parameters calculated for the active medium of the oxygen-iodine laser in the transverse section of a gas flow where the gain coefficient reaches a maximum. The calculations are made in model III for $T_0 = 300$ K and the composition of the medium $O_2 : O_2(^1\Delta) : H_2O : I_2 : N_2 = 1000 : 700 : m : n : 0$.

m	n	$\alpha_p^{\max}/m^{-1} \text{ Torr}^{-1}$	$\tau^{\max}/\text{ms Torr}$	η_A^{\max}	ϕ^{\max}	l^{\max}
0	1	0.035	4.00	0.69	0.04	1.11
	2	0.068	2.30	0.69	0.04	1.12
	5	0.158	1.13	0.68	0.04	1.15
	10	0.280	0.65	0.66	0.05	1.21
	20	0.446	0.40	0.63	0.05	1.34
	40	0.578	0.23	0.59	0.09	1.56
10	1	0.033	4.00	0.69	0.06	1.13
	2	0.063	2.40	0.68	0.06	1.14
	5	0.146	1.20	0.67	0.06	1.19
	10	0.258	0.70	0.66	0.06	1.25
	20	0.404	0.40	0.63	0.09	1.37
	40	0.518	0.23	0.59	0.16	1.59
50	1	0.026	4.20	0.68	0.15	1.20
	2	0.049	2.70	0.68	0.15	1.24
	5	0.110	1.40	0.67	0.16	1.30
	10	0.188	0.80	0.65	0.20	1.36
	20	0.286	0.48	0.63	0.23	1.50
	40	0.362	0.27	0.60	0.36	1.68
100	1	0.021	4.40	0.67	0.24	1.27
	2	0.038	2.80	0.67	0.28	1.30
	5	0.081	1.53	0.66	0.30	1.38
	10	0.135	0.95	0.65	0.33	1.47
	20	0.202	0.52	0.63	0.43	1.54
	40	0.260	0.30	0.61	0.54	1.70
200	1	0.015	4.00	0.67	0.42	1.31
	2	0.025	2.80	0.67	0.47	1.37
	5	0.050	1.60	0.66	0.53	1.44
	10	0.082	1.00	0.65	0.58	1.50
	20	0.123	0.60	0.64	0.65	1.59
	40	0.163	0.33	0.63	0.73	1.66

esses forming inverse population on transitions of the iodine atom. Fig. 3 presents an example of the calculation of population of the first vibrational level of the oxygen molecule in conditions typical of the COL. One can see that vibrational quanta are accumulated on the first vibrational level of oxygen with time. In this specific example, the vibrational population of oxygen for $\tau = 2$ ms Torr reaches 38%. The presence of a region with population inversion whose length along the flow is sufficiently large is one of the conditions for applying laser cavities that provide a sharp directivity of radiation in a COL. In this case, several tens of percent of oxygen molecules at the output of a COL cavity may be vibrationally populated.

Vibrationally excited oxygen will be involved in the kinetics of forming inverse population of iodine atoms in reaction 21, which is similar to reaction 3 (see Table 1). As follows from calculations, the proportion of vibrationally excited oxygen in a mixture is of considerable importance, and, therefore, one should take this process into account when modeling the COL.

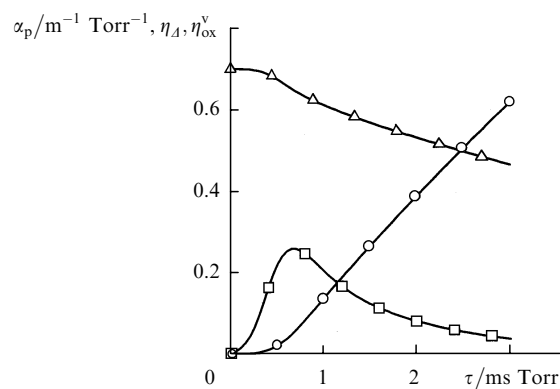


Figure 3. Dependences of the gain coefficient of a medium (\square), the fraction of singlet oxygen (Δ), and the fraction of $O_2(v=1)\eta_{ox}^v$ (\circ) on τ calculated for $T_0 = 300$ K and the medium with composition $O_2 : O_2(^1\Delta) : H_2O : I_2 : N_2 = 1000 : 700 : 50 : 20 : 0$ in dissociation model IV.

4. Conclusions

Thus, our analysis of the models of I_2 dissociation in the oxygen-iodine medium showed that models III and IV give approximately the same iodine dissociation rate in a wide range of compositions of the oxygen-iodine medium. Iodine dissociation at the initiation stage in reactions 5b (model III) and 5c (model IV) has the same rates. In model IV, iodine dissociation at the initiation and chain stages is described by one and the same reactions, and this is its advantage over model III. The rate of decrease in vibrational energy accumulated due to the relaxation of electronic energy in oxygen is limited by the rate of VV energy exchange between oxygen and water molecules. Our estimation of the rate constant of this process gave $K_{13} \approx 3 \times 10^{-13} \text{ cm}^3 \text{ s}^{-1}$.

Approximately 2% of oxygen molecules at the output of the jet-droplet generator of singlet oxygen are found on the first vibrationally excited level. The vibrational population of oxygen in the active medium of the COL can reach several tens of percent. Because of this, vibrational processes make a substantial contribution to the formation of population inversion on the atomic iodine transition, and one should take them into account when modeling the COL.

References

1. Heidner III R F, Gardner C E, Segal G I, El-Sayed T M *J. Phys. Chem.* **87** 2348 (1983)
2. Heidner III R F, Gardner C E, El-Sayed G I, Segal T M *Chem. Phys. Lett.* **81** 142 (1981)
3. Arnold S J, Finlayson N, Ogruzlo E A *J. Chem. Phys.* **44** 2529 (1966)
4. Derwent R G, Trush B A *Trans. Faraday Soc.* **67** 2036 (1971)
5. Derwent R G, Trush B A *J. Chem. Soc. Faraday Trans. II* **68** 720 (1972)
6. Derwent R G, Trush B A *Faraday Discuss. Chem. Soc.* **53** 162 (1972)
7. Muller D F, Young R H, Houston P L, Wiesenfeld J R *Appl. Phys. Chem.* **38** 404 (1981)
8. Baramashenko B D, Rosenwaks S *AIAA J.* **34** 2569 (1996)
9. Marter T, Heaven M C, Plummer D *Chem. Phys. Lett.* **260** 201 (1996)
10. Cline J I, Leone S R *J. Phys. Chem.* **95** 2917 (1991)
11. Azyazov V N, Igoshin V I, Kupriyanov N L *Kratkie Soobshch. Fiz. FIAN* No. 1–2 24 (1992)
12. Aviles R G, Muller D F, Houston P L *Appl. Phys. Lett.* **37** 358 (1980)

13. Collins R J, Husain D J. *Photochem.* **1** 481 (1972)
14. Bloemink H I, Copeland R A, Slander T G J. *Chem. Phys.* **109** 4237 (1998)
15. Parker J G, Ritke D N J. *Chem. Phys.* **59** 3713 (1973)
16. Britan A B, Starik A M. *Zh. Prikl. Mekh. Tekh. Fiz.* No. 4 41 (1980)
17. Finzi J, Hovis F E J. *Chem. Phys.* **67** 4053 (1977)
18. Fisk G A, Hays G N J. *Chem. Phys.* **77** 4985 (1982)
19. Burde D H, McFarlane R A J. *Chem. Phys.* **64** 1850 (1976)
20. Hall G E, Marne W J, Houston P L J. *Phys. Chem.* **87** 2153 (1983)
21. Van Bethem M H, Davis S J J. *Phys. Chem.* **90** 902 (1986)
22. Barnault B, Bouvier A J, Pigashe D, Bacis R. *Laser M2P* (Grenoble, 1991)
23. Didyukov A I, Kulagin Yu A, Shelepin L A, Yarygina V N. *Kvantovaya Elektron. (Moscow)* **16** 892 (1989) [*Sov. J. Quantum Electron.* **19** 578 (1989)]
24. Biryukov A S, Shcheglov V A. *Kvantovaya Elektron. (Moscow)* **13** 511 (1986) [*Sov. J. Quantum Electron.* **16** 334 (1986)]
25. Borrell P M, Borrell P, Grant K R. *J. Chem. Soc. Faraday Trans.* **76** 923 (1980)
26. Boodaghians R, Borrell P M, Borrell P, Grant K R. *J. Chem. Soc. Faraday Trans.* **78** 1195 (1982)
27. Azyazov V N, Nikolaev V D, Svistun M I, Ufimtsev N I. *Kvantovaya Elektron. (Moscow)* **28** 212 (1999) [*Quantum Electron.* **29** 767 (1999)]
28. Schurath U J. *Photochem.* **4** 215 (1975)